



**HAL**  
open science

## Time-resolved resonance fluorescence spectroscopy for study of chemical reactions in laser-induced plasmas

Lei Liu, Lei Min Deng, Li Sha Fan, Xi Huang, Yao Lu, Xiaokang Shen, Lan Jiang, Jean-François Silvain, Yongfeng Lu

► **To cite this version:**

Lei Liu, Lei Min Deng, Li Sha Fan, Xi Huang, Yao Lu, et al.. Time-resolved resonance fluorescence spectroscopy for study of chemical reactions in laser-induced plasmas. *Optics Express*, 2017, 25 (22), pp.27000-27007. 10.1364/OE.25.027000 . hal-01662370

**HAL Id: hal-01662370**

**<https://hal.science/hal-01662370>**

Submitted on 14 Sep 2020

**HAL** is a multi-disciplinary open access archive for the deposit and dissemination of scientific research documents, whether they are published or not. The documents may come from teaching and research institutions in France or abroad, or from public or private research centers.

L'archive ouverte pluridisciplinaire **HAL**, est destinée au dépôt et à la diffusion de documents scientifiques de niveau recherche, publiés ou non, émanant des établissements d'enseignement et de recherche français ou étrangers, des laboratoires publics ou privés.



# Time-resolved resonance fluorescence spectroscopy for study of chemical reactions in laser-induced plasmas

LEI LIU,<sup>1</sup> LEIMIN DENG,<sup>1</sup> LISHA FAN,<sup>1</sup> XI HUANG,<sup>1</sup> YAO LU,<sup>1</sup> XIAOKANG SHEN,<sup>1</sup> LAN JIANG,<sup>2</sup> JEAN-FRANÇOIS SILVAIN,<sup>1,3</sup> AND YONGFENG LU<sup>1,\*</sup>

<sup>1</sup>Department of Electrical and Computer Engineering, University of Nebraska-Lincoln, Lincoln, NE 68588-0511, USA

<sup>2</sup>School of Mechanical Engineering, Beijing Institute of Technology, 100081, China

<sup>3</sup>Institut de Chimie de la Matière Condensée de Bordeaux-ICMCB-CNRS 87, Avenue du Docteur Albert Schweitzer F-33608 Pessac Cedex, France

\*ylu2@unl.edu

**Abstract:** Identification of chemical intermediates and study of chemical reaction pathways and mechanisms in laser-induced plasmas are important for laser-ablated applications. Laser-induced breakdown spectroscopy (LIBS), as a promising spectroscopic technique, is efficient for elemental analyses but can only provide limited information about chemical products in laser-induced plasmas. In this work, time-resolved resonance fluorescence spectroscopy was studied as a promising tool for the study of chemical reactions in laser-induced plasmas. Resonance fluorescence excitation of diatomic aluminum monoxide (AlO) and triatomic dialuminum monoxide (Al<sub>2</sub>O) was used to identify these chemical intermediates. Time-resolved fluorescence spectra of AlO and Al<sub>2</sub>O were used to observe the temporal evolution in laser-induced Al plasmas and to study their formation in the Al-O<sub>2</sub> chemistry in air.

© 2017 Optical Society of America

**OCIS codes:** (300.2530) Fluorescence, laser-induced; (300.6390) Spectroscopy, molecular.

## References and links

1. Y. T. Su, Y. H. Huang, H. A. Witek, and Y. P. Lee, "Infrared Absorption Spectrum of the Simplest Criegee Intermediate CH<sub>2</sub>OO," *Science* **340**(6129), 174–176 (2013).
2. H. Hou, X. Mao, V. Zorba, and R. E. Russo, "Laser Ablation Molecular Isotopic Spectrometry for Molecules Formation Chemistry in Femtosecond-Laser Ablated Plasmas," *Anal. Chem.* **89**(14), 7750–7757 (2017).
3. G. Jian, N. W. Piekielek, and M. R. Zachariah, "Time-Resolved Mass Spectrometry of Nano-Al and Nano-Al/CuO Thermite under Rapid Heating: A Mechanistic Study," *J. Phys. Chem. C* **116**, 26881–26887 (2012).
4. L. Zhou, N. Piekielek, S. Chowdhury, and M. R. Zachariah, "Time-Resolved Mass Spectrometry of the Exothermic Reaction between Nanoaluminum and Metal Oxides: The Role of Oxygen Release," *J. Phys. Chem. C* **114**, 14269–14275 (2010).
5. Z. Miao, H. Chen, P. Liu, and Y. Liu, "Development of Submillisecond Time-Resolved Mass Spectrometry Using Desorption Electrospray Ionization," *Anal. Chem.* **83**(11), 3994–3997 (2011).
6. M. L. Alexander, M. R. Smith, J. S. Hartman, A. Mendoza, and D. W. Koppenaal, "Laser ablation inductively coupled plasma mass spectrometry," *Appl. Surf. Sci.* **127**, 255–261 (1998).
7. A. W. Miziolek, V. Palleschi, and I. Schechter, *Laser-induced Breakdown Spectroscopy (LIBS): Fundamentals and Applications* (Cambridge University Press, 2006).
8. J. P. Singh and S. N. Thakur, *Laser-induced Breakdown Spectroscopy* (Elsevier, 2007).
9. E. N. Rao, S. Sunku, and S. V. Rao, "Femtosecond Laser-Induced Breakdown Spectroscopy Studies of Nitropyrazoles: The Effect of Varying Nitro Groups," *Appl. Spectrosc.* **69**(11), 1342–1354 (2015).
10. A. A. Bol'shakov, X. L. Mao, J. Jain, D. L. McIntyre, and R. E. Russo, "Laser ablation molecular isotopic spectrometry of carbon isotopes," *Spectrochim. Acta B At. Spectrosc.* **113**, 106–112 (2015).
11. X. L. Mao, A. A. Bol'shakov, I. Choi, C. P. McKay, D. L. Perry, O. Sorkhabi, and R. E. Russo, "Laser Ablation Molecular Isotopic Spectrometry: Strontium and its isotopes," *Spectrochim. Acta B At. Spectrosc.* **66**, 767–775 (2011).
12. X. L. Mao, A. A. Bol'shakov, D. L. Perry, O. Sorkhabi, and R. E. Russo, "Laser Ablation Molecular Isotopic Spectrometry: Parameter influence on boron isotope measurements," *Spectrochim. Acta B At. Spectrosc.* **66**, 604–609 (2011).
13. R. E. Russo, A. A. Bol'shakov, X. L. Mao, C. P. McKay, D. L. Perry, and O. Sorkhabi, "Laser Ablation Molecular Isotopic Spectrometry," *Spectrochim. Acta B At. Spectrosc.* **66**, 99–104 (2011).

14. A. Sarkar, X. L. Mao, G. C. Y. Chan, and R. E. Russo, "Laser ablation molecular isotopic spectrometry of water for 1 D2/1 H1 ratio analysis," *Spectrochim. Acta B At. Spectrosc.* **88**, 46–53 (2013).
15. M. Sarvan, M. Perić, L. Zeković, S. Stojadinović, I. Belča, M. Petković, and B. Kasalica, "Identification of the C2II-X2Σ+ band system of AlO in the ultraviolet galvanoluminescence obtained during aluminum anodization," *Spectrochim. Acta A Mol. Biomol. Spectrosc.* **81**(1), 672–678 (2011).
16. M. Singh and M. D. Saksena, "C 2IIr – X 2Σ+ Transition of AlO," *Can. J. Phys.* **61**, 1347–1358 (1983).
17. M. D. Saksena, M. N. Deo, K. Sunanda, S. H. Behere, and C. T. Londhe, "Fourier transform spectral study of B 2Σ+ – X 2Σ+ system of AlO," *J. Mol. Spectrosc.* **247**, 47–56 (2008).
18. C. G. Parigger and J. O. Hornkohl, "Computation of AlO B2Σ+ → X2Σ+ emission spectra," *Spectrochim. Acta A Mol. Biomol. Spectrosc.* **81**(1), 404–411 (2011).
19. A. T. Patrascu, C. Hill, J. Tennyson, and S. N. Yurchenko, "Study of the electronic and rovibronic structure of the X 2Σ+, A 2Π, and B 2Σ+ states of AlO," *J. Chem. Phys.* **141**(14), 144312 (2014).
20. E. Wagner, "Ab initio versus CNDO potential surface calculations for Li<sub>2</sub>O and Al<sub>2</sub>O," *Theor. Chem. Acc.* **32**, 295–310 (1974).
21. M. F. Cai, C. C. Carter, T. A. Miller, and V. E. Bondybey, "Fluorescence Excitation and Resolved Emission-Spectra of Supersonically Cooled Al<sub>2</sub>O," *J. Chem. Phys.* **95**, 73–79 (1991).
22. J. Koput and A. Gertych, "Ab initio prediction of the potential energy surface and vibrational-rotational energy levels of dialuminum monoxide, Al<sub>2</sub>O," *J. Chem. Phys.* **121**(1), 130–135 (2004).
23. J. M. Turney, L. Sari, Y. Yamaguchi, and H. F. Schaefer, "The singlet electronic ground state isomers of dialuminum monoxide: AlOAl, AlAlO, and the transition state connecting them," *J. Chem. Phys.* **122**(9), 094304 (2005).
24. J. Masip, A. Clotet, J. Ricart, F. Illas, and J. Rubio, "Molecular structure and vibrational frequencies of Al<sub>x</sub>O<sub>y</sub> (x= 1, 2; y ≤ 3) derived from ab initio calculations," *Chem. Phys. Lett.* **144**, 373–377 (1988).
25. M. A. Douglas, R. H. Hauge, and J. L. Margrave, "Electronic Absorption and Emission Studies of the Group-IIia Metal Suboxides Isolated in Cryogenic Rare-Gas Matrices," *High Temp. Sci.* **16**, 35–54 (1983).
26. G. I. Pangilinan and T. P. Russell, "Role of Al-O<sub>2</sub> chemistry in the laser-induced vaporization of Al films in air," *J. Chem. Phys.* **111**, 445–448 (1999).
27. M. V. Pak and M. S. Gordon, "Potential energy surfaces for the Al + O<sub>2</sub> reaction," *J. Chem. Phys.* **118**, 4471–4476 (2003).

## 1. Introduction

Identification of chemical intermediates and the study of chemical reaction pathways and mechanisms in laser-induced plasmas are important for laser material interactions but present challenges. Both optical spectroscopy and mass spectrometry (MS) analytical methodologies have been used for studies of chemistry in laser-induced vapors, such as infrared (IR) spectroscopy [1], molecular emission spectroscopy (MES) [2], time-resolved mass spectrometry (TRMS) [3–5], and inductively coupled plasma-mass spectrometry (ICP-MS) [6]. Analytical techniques capable of characterizing molecular species in time are necessary for studying chemical reactions. Time resolution is a key parameter of the technique used. Time-resolved MS is one of the main techniques in chemical analyses due to its capability of identifying molecules and clusters along with evaluating temporal evolution and high sensitivity. However, optical spectroscopy has the characteristic advantages of superior temporal resolution, in situ analysis, applicable for extensive atmospheric environments (such as open air, inert gases, or reactive gases) at different pressures, for solid, liquid, and gas analyses, etc.

Laser-induced breakdown spectroscopy (LIBS) as one of the spectroscopic techniques for chemical analyses has the advantages of nearly nondestructive, in situ real-time analyses; remote detection; trace element analyses; and active all-element detection, etc., but is mainly used for elemental analyses [7]. The laser-ablated materials undergo the processes in a time sequence of vaporization, ionization/atomization, and recombination; and these excited species emit at their characteristic wavelengths [8]. LIBS mainly takes advantage of the ionic/atomic emissions for chemical analyses. Recently, molecular emission in the laser-induced plasmas has attracted great interest for organic compounds recognition [9], diatomic molecule identification, isotope determination [10–14], and isotope-labeled chemistry for the study of diatomic molecule formation [2]. Generally, a gate width in the submicrosecond scale is necessary for molecular emission measurements due to the relatively low emission intensity compared with atomic/ionic emissions in the laser-induced plasma. Also, only

diatomic molecular emission bands with relatively large electronic transition probability are used for measurements and analyses.

In this work, resonance fluorescence excitation was proposed to identify both diatomic and polyatomic chemical intermediates in laser-induced plasmas. Time-resolved fluorescence spectra were used to study temporal evolution of the chemical intermediates as a potential tool for chemical reaction pathway analyses. One advantage of resonance fluorescence excitation of molecules is that a small gate width, down to a few nanoseconds (ns), could be used to acquire high-quality spectra for analyses, which would significantly improve the temporal resolution of this technique and make it promising for chemical reaction analyses. In addition, for polyatomic molecules with naturally weak emissions in the ultraviolet-visible spectroscopy (UV-VIS) range, fluorescence emissions can be significantly excited and easy to measure by resonance excitations. Besides, the selective resonance excitation can significantly reduce spectral interference from other chemical products, which is desirable for analyses of chemical reactions in laser-induced plasmas with various chemical products. Also, resonance fluorescence spectroscopy maintains the characteristic advantages of optical spectroscopy technology and can easily cooperate with other optical spectroscopic techniques for more complicated analyses or specific applications. In this work, we chose aluminum (Al) as a sample for studying the temporal evolution of two important chemical intermediates, aluminum monoxide (AlO) and dialuminum monoxide (Al<sub>2</sub>O), in the Al-O<sub>2</sub> chemistry. This approach can easily be extended to other diatomic and polyatomic molecules. Benefits of this approach are rapid molecule identification (which is complementary to LIBS), temporal evolution monitoring of diatomic and polyatomic molecules as a potential tool for chemical reaction pathways and mechanisms analyses, and significantly improved temporal resolution for chemical reaction analyses with gate widths for detection down to a few nanoseconds.

## 2. Experiment setup

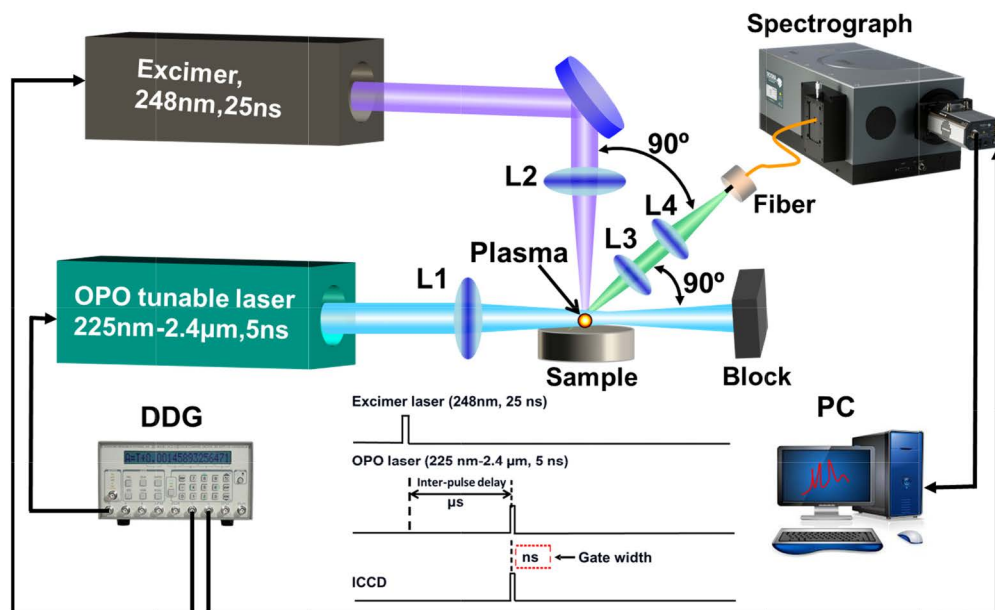


Fig. 1. Schematic diagram of the experiment setup.

The schematic diagram of the experiment setup is shown in Fig. 1. A KrF Excimer laser (Coherent Inc., COMPex 205, 25ns) with a wavelength of 248 nm and a repetition rate of 10 Hz was used for laser ablation of an Al sample. The laser has an energy of 190 mJ/pulse and was focused to a spot size of 1 mm × 3 mm on the sample surface by Lens 1 ( $f_1 = 20$  cm). A

wavelength tunable optical parametric oscillator (OPO) laser (OPOTEK Inc., VIBRANT 355 LD, 5 ns, 0.22–2.4  $\mu\text{m}$ , spectral linewidth 4–7  $\text{cm}^{-1}$ ) was slightly defocused on the plasma by Lens 2 ( $f_2 = 10$  cm) to a spot size of 3 mm in diameter. The measured spectrum signals are the spatially integrated resonance fluorescence emission. The wavelength of the probe laser was tuned to selectively excite the electronic transitions of diatomic AlO and triatomic  $\text{Al}_2\text{O}$  molecules in the laser-induced plasmas in air. The probe laser energy was 5 and 2 mJ/pulse for resonance fluorescence excitation of AlO and  $\text{Al}_2\text{O}$ , respectively, with the maximum output power at different wavelengths. The interpulse delay time between the ablation and probe laser pulses was controlled by a digital delay generator (Stanford Research Systems DG535, 5 ps delay resolution). A pair of convex lenses ( $f_3 = 10$  cm,  $f_4 = 6$  cm) were used to collect and couple the resonance fluorescence emissions from the excited molecules to an optical fiber. The optical fiber then coupled the collected emission signals into a spectrometer (Andor Technology, Shamrock 505i, ICCD DT-334T) for measurement. The pair of lenses used for collecting light from plasma emission was put in plane with the probe laser beam and vertical to its direction. The intensified charge-coupled device (ICCD) detector was temporally synchronized with the probe laser pulse. For data acquisition, resonance fluorescence spectra and time-resolved fluorescence spectra of AlO and  $\text{Al}_2\text{O}$  were acquired. For resonance fluorescence spectrum measurement, a gate width of 10 ns, an accumulation of 100 pulses, and a fixed interpulsed delay time of 20  $\mu\text{s}$  were used. For time-resolved fluorescence spectrum measurement, a gate width of 10 ns, an accumulation of 30 pulses, and an increase step of 2  $\mu\text{s}$  in interpulse delay time were used.

### 3. Results and discussion

#### 3.1 Resonance fluorescence excitation of AlO

For the diatomic AlO, the electronic and rovibronic structures have been extensively studied [2, 17–19]. In this work, we resonantly excited the naturally weak emission from the  $\text{C}^2\Pi_r\text{--X}^2\Sigma^+$  electronic transition system of AlO. The  $\text{C}^2\Pi_r\text{--X}^2\Sigma^+$  transition system has been studied both by experiment [16] and theoretical calculation [15] with the detailed band origins listed in Table 1, which is cited from Refs [15, 16]. In Refs [15, 16], the data for band origins are shown in the unit of  $\text{cm}^{-1}$ . In order to clearly show the excitation and transition processes in this work, the corresponding data with the unit of nm are also shown in Table 1, obtained by direct  $\text{cm}^{-1}$  to nm unit conversion. In this study, resonance fluorescence excitation of vibrational transitions in the  $\Delta v = 0$  band of the  $\text{C}^2\Pi_r\text{--X}^2\Sigma^+$  electronic transition system of AlO were conducted. The fluorescence spectra of AlO with the excitation wavelength at 302.13, 302.94, 303.30, and 304.00 nm are shown in Fig. 2(a)–2(d), respectively. Figure 2 shows that, for resonance excitation of vibrational transitions in the  $\Delta v = 0$  band, the corresponding vibrational transitions in the  $\Delta v = \pm 1$  were significantly excited. For example, with the excitation wavelengths at 302.13 and 302.94 nm with resonance to the (0-0) vibrational transitions of  $\text{C}^2\Pi_{3/2}(\text{F}_2)\text{--X}^2\Sigma^+$  and  $\text{C}^2\Pi_{1/2}(\text{F}_1)\text{--X}^2\Sigma^+$ , the corresponding (0-1) vibrational transitions at 311.26 and 312.09 nm were significantly excited and observed, as shown in Fig. 2(a) and 2(b), respectively. Similarly, with the excitation wavelength at 303.30 and 304.00 nm with resonance to the (1-1) vibrational transitions of  $\text{C}^2\Pi_{3/2}(\text{F}_2)\text{--X}^2\Sigma^+$  and  $\text{C}^2\Pi_{1/2}(\text{F}_1)\text{--X}^2\Sigma^+$ , the corresponding  $\Delta v = \pm 1$  vibrational transitions were observed with the (1-2) transitions at 312.39 and 313.08 nm and (1-0) transitions at 294.73 and 295.44 nm, as shown in Fig. 2(c) and 2(d), respectively. The observed resonance excitations and fluorescence emissions were consistent with previous studies [15, 16] and were used to identify the existence of AlO in the laser-induced plasmas.

Table 1. Band origins of the  $C^2\Pi_u - X^2\Sigma^+$  transition of  $AlO$ . Cited from Refs [15, 16].

Band ( $v'u''$ )	$C^2\Pi_{1/2}(F_1) - X^2\Sigma^+$ Transition		$C^2\Pi_{3/2}(F_2) - X^2\Sigma^+$ Transition		
	nm	$cm^{-1}$	nm	$cm^{-1}$	
$\Delta v = 0$	0-0	302.9385	33010	33098	
	1-1	304.0068	32894	303.3244	32968
$\Delta v = -1$	0-1	312.0612	32045	311.2162	32132
	1-2	313.0576	31943	312.3438	32016
	2-3	314.0802	31839	313.2538	31923
$\Delta v = 1$	1-0	295.3425	33859	294.3984	33933
	2-1	296.5160	33725	295.8667	33799
	3-2	297.6634	33595	296.9210	33679

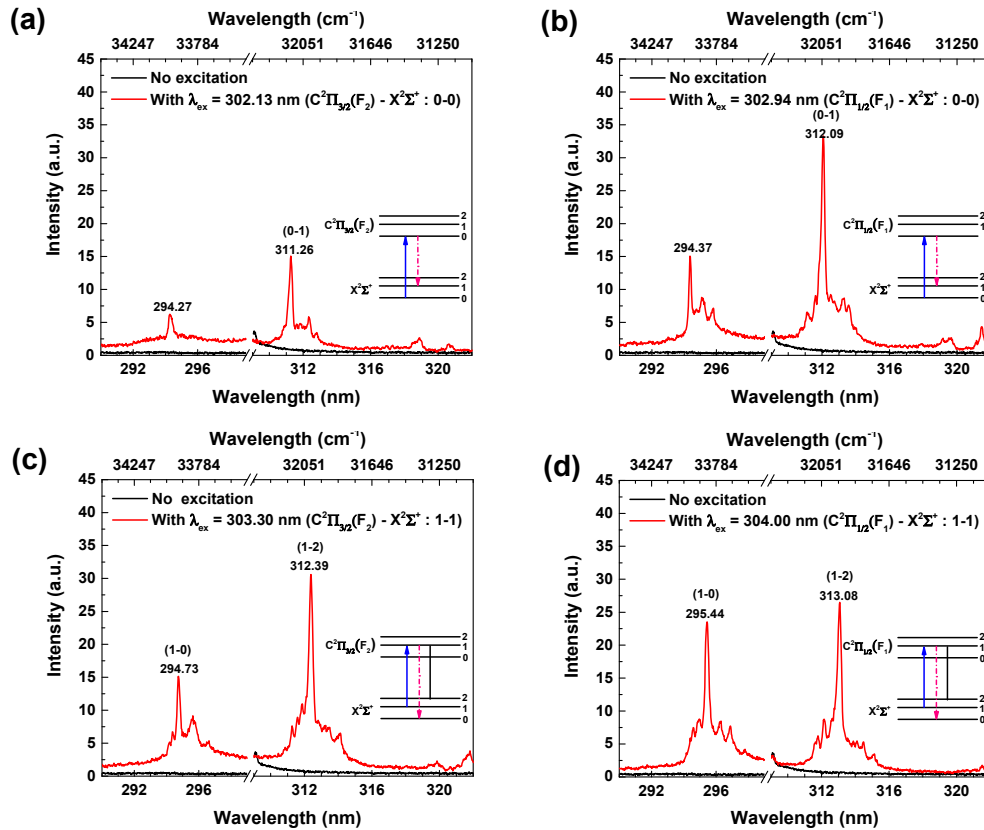


Fig. 2. Resonance fluorescence spectra with the excitation wavelengths at (a) 302.13, (b) 302.94, (c) 303.30, and (d) 304.00 nm measured with a gate width of 10 ns, an accumulation of 100 pulses, and a fixed interspersed delay time of 20  $\mu s$ .

### 3.2 Resonance fluorescence excitation of $Al_2O$

For the triatomic molecule,  $Al_2O$ , spectroscopic studies about its electronic structures have been studied [20–25]; but assignment of the vibrational structures in terms of electronic states has not been completed due to its complexity. Fluorescence excitation of gas-phase  $Al_2O$  in laser-induced vapor has been conducted experimentally by Cai [21]; and a broad range fluorescence emission in the range of 38000–40200  $cm^{-1}$  (248–263 nm) from  $^1\Pi_u \rightarrow X^1\Sigma_g^+$  electronic structure transition was observed with strong emission bands at around 38200–38400  $cm^{-1}$  (260–261 nm), 39000–39600  $cm^{-1}$  (252–266 nm), and 39800–40000  $cm^{-1}$  (250–

251 nm). In this study, several excitation wavelengths in the referenced fluorescence spectral ranges were used to resonantly excite fluorescence emission of  $\text{Al}_2\text{O}$ . The measured fluorescence spectra of  $\text{Al}_2\text{O}$  with the excitation wavelengths at 250.14, 255.10, 255.38, and 261.40 nm are shown in Fig. 3(a)–3(d), respectively. The curves in Fig. 3(d) have been magnified three times for clear display.

At different excitation wavelengths, different vibrational structures were excited. For example, with the excitation wavelength at 250.14 nm, the emission bands centered at 255 and 260 nm were excited. With the excitation wavelength at 255.38 and 256.00 nm, the emission bands centered at 250 and 260 nm were excited. With the excitation wavelength at 261.40 nm, the emission bands centered at 255 nm were excited. These emission bands observed match the previously observed fluorescence emissions of  $\text{Al}_2\text{O}$  by Cai [21] in this broad wavelength range and were used to identify the triatomic  $\text{Al}_2\text{O}$  in laser-induced plasmas in this work.

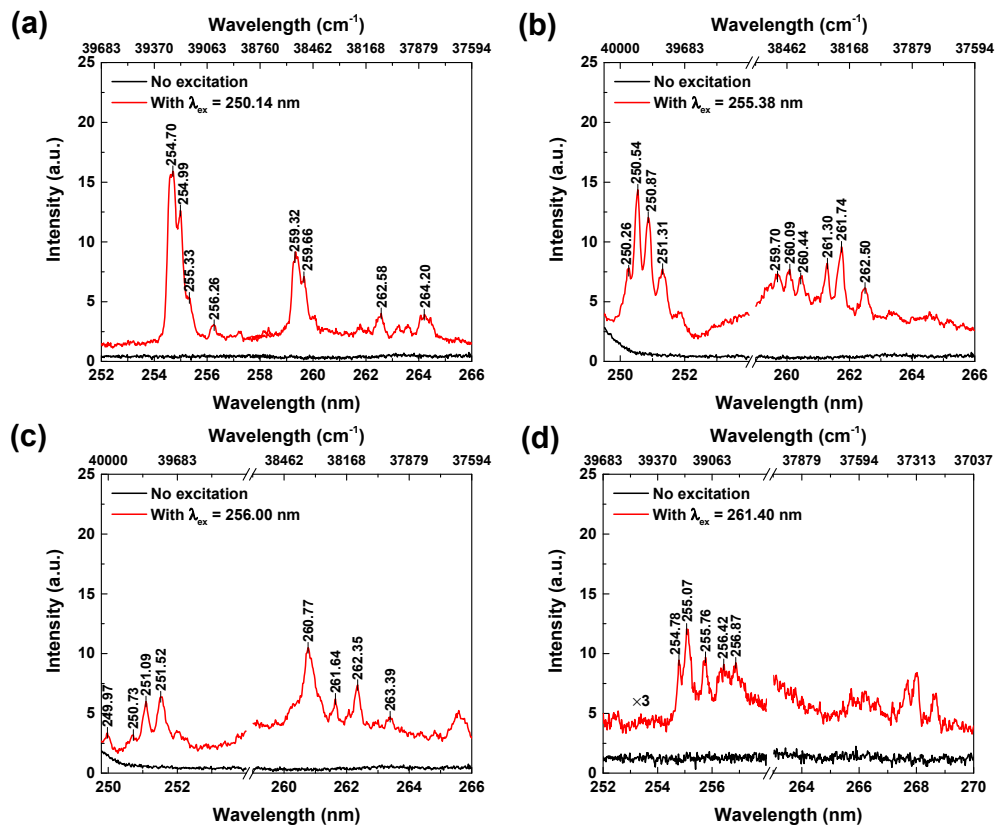


Fig. 3. Resonance fluorescence spectra of  $\text{Al}_2\text{O}$  with the excitation wavelengths at (a) 250.14, (b) 255.38, (c) 256.00, and (d) 261.40 nm measured with a gate width of 10 ns, an accumulation of 100 pulses, and a fixed interpulse delay time of 20  $\mu\text{s}$ .

### 3.3 Temporal evolution of $\text{AlO}$ and $\text{Al}_2\text{O}$ in resonance fluorescence spectra

For laser-induced Al plasmas in air,  $\text{AlO}$  and  $\text{Al}_2\text{O}$  are two important chemical intermediates in the  $\text{Al-O}_2$  chemistry described by the following chemical reactions [3, 21, 26, 27]:



In this work, time-resolved resonance fluorescence spectra were measured to observe the temporal evolution of AlO and Al<sub>2</sub>O in the Al-O<sub>2</sub> chemistry. Time-resolved fluorescence intensities of AlO (peak intensity at 313.08 nm with a resonance excitation at 304.00 nm) and Al<sub>2</sub>O (peak intensity at 261.40 nm with a resonance excitation at 256.00 nm) were observed with a gate width of 10 ns and a gate step of 2 μs, as shown in Fig. 4. The temporal evolution of atomic line intensities of Al I 308.2 nm and O I 777.2 nm were also measured with a gate width of 1 μs and a gate step of 1 μs. All of these optical emission intensities were normalized to their maximum value. Both the Al and O atomic emissions decrease rapidly along with the delay time due to plasma cooling, but the O temporal evolution profile has a faster decrease due to its high chemical reactivity. Chemical intermediates were formed during the atoms/ions cool-down process. The temporal profile of AlO dominates the time range of around 10-40 μs, while the temporal profile of Al<sub>2</sub>O dominates the later time range of around 20-50 μs. The temporal profile of AlO shows that the AlO concentration increases in the time range of around 10-30 μs followed by a decrease due to dissipation or further chemical reactions. While the increase section of the Al<sub>2</sub>O temporal profile occurs later than that of AlO, so does the decrease section, which indicates that a large amount of Al<sub>2</sub>O formation occurs later than that of AlO in the chemical reactions. This is consistent with the previously demonstrated chemical reaction pathways, as shown in Eqs. (1) and (2). The Al atoms react with surrounding O<sub>2</sub> to form AlO via the chemical reaction pathway, as shown in Eq. (1) [2]. Due to the abundance of Al atoms, the AlO undergoes a reduction and further formation of Al<sub>2</sub>O through the chemical reaction pathway, as shown in Eq. (2). That is why the dominate time range of the Al<sub>2</sub>O temporal profile occurs later than that of AlO. Therefore, time-resolved fluorescence spectra can be considered as a potential tool for the study of chemical reaction pathways for diatomic and polyatomic molecules.

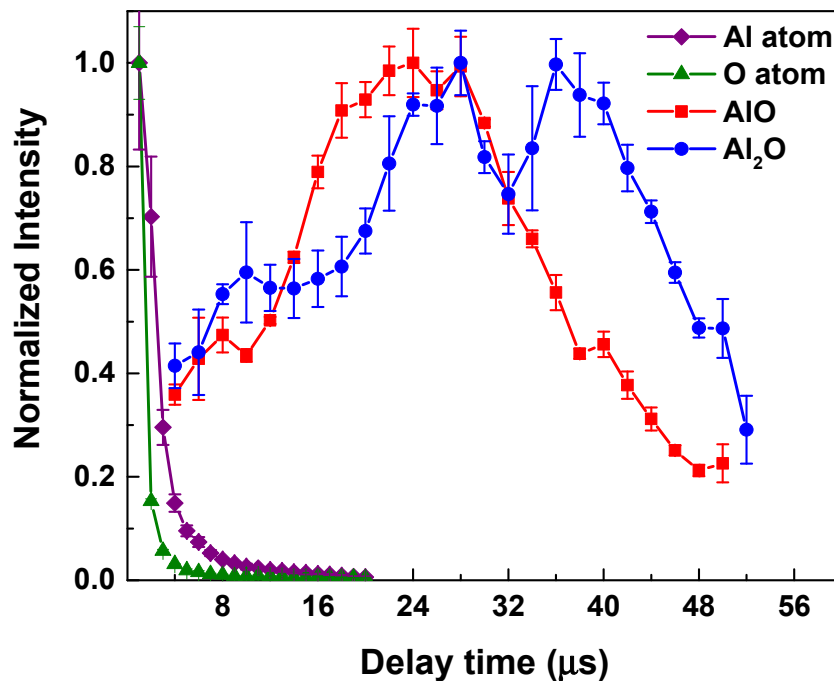


Fig. 4. Temporal evolution of the normalized emission intensities of Al I 308.2 nm (diamond dots), O I 777.2 nm (triangle dots), AlO 313.08 nm (square dots), and Al<sub>2</sub>O 261.40 nm (circle dots).

#### 4. Conclusions

Time-resolved resonance fluorescence spectroscopy was performed as a promising tool for the study of chemical reaction pathways for diatomic and polyatomic molecules in laser-induced plasmas. Resonance fluorescence spectroscopy provides the advantages of superior temporal resolution with the gate widths for detection down to a few ns and selective excitation to eliminate spectral interference from other chemical products, which are promising for chemical reaction analyses of laser-induced plasmas in air where various chemical species exist. For laser-induced Al plasmas in air, resonance fluorescence spectra from diatomic AlO ( $C^2\Pi_r-X^2\Sigma^+$ ) and triatomic Al<sub>2</sub>O ( $^1\Pi_u \rightarrow X^1\Sigma_g^+$ ) were used to identify these chemical intermediates. Time-resolved fluorescence spectra were measured to construct normalized temporal profiles for study of chemical reaction pathways. The temporal profile of Al<sub>2</sub>O dominates a later time range than that of AlO, which indicates a large amount of Al<sub>2</sub>O formation occurred later than that of AlO. This conclusion is consistent with previous studies [3, 26, 27] that AlO formation follows the chemical reaction pathway of  $Al + O_2 \rightarrow AlO + O$  and Al<sub>2</sub>O formation follows the chemical reaction pathway of  $AlO + Al \rightarrow Al_2O$  in Al-abundant environments.

#### Funding

Defense Threat Reduction Agency (DTRA) (HDTRA1-12-1-0019, HDTRA1-13-1-0019).

#### Acknowledgements

Lei Liu and Leimin Deng contributed equally to this work. The research was performed partially in the Nebraska Nanoscale Facility: National Nanotechnology Coordinated Infrastructure and the Nebraska Center for Materials and Nanoscience, which are supported by National Science Foundation and the Nebraska Research Initiative.